Progress In Electromagnetics Research, Vol. 132, 403–424, 2012

SCATTERING OF AN ARBITRARILY ORIENTED DIPOLE FIELD BY A CIRCULAR DISK WITH SURFACE IMPEDANCE

A. D. U. Jafri[1], Q. A. Naqvi[1, *], A. A. Syed[1], and K. Hongo[2]

[1]Department of Electronics, Quaid-i-Azam University, Islamabad, Pakistan

[2]3-34-24, Nakashizu, Sakura City, Chiba, Japan

Abstract—The scattering of an arbitrarily oriented dipole field by a circular disk with surface impedance is investigated by using the method of Kobayashi Potential (KP method). The dual integral equations (DIE) are produced during formulation of the problem. The solution of the DIEs is constructed in terms of set of functions which satisfy the boundary conditions as well as required edge conditions. At this stage, we applied the discontinuous properties of Weber Schafheitlins integral and vector Hankel transform. After applying the projection, the resulting expressions are reduced to the matrix equations for the expansion coefficients. The matrix elements are given in terms of the infinite integrals. The far field patterns for the scattered wave are computed for different incident angles, disk sizes and surface impedances for ρ-, ϕ- and z-directed dipole field excitation. To validate the results we have obtained the results based on the physical optics approximation and their comparison shows that they quite reasonably match.

1. INTRODUCTION

The circular disk being a classical scatterer in the field of electromagnetics has received much attention for a long time. The solution of electromagnetic scattering problems satisfies the Maxwell equations and boundary conditions. The surfaces with large conductivity can be treated with surface impedance boundary condition. The use of surface impedance boundary condition (SIBC)

Received 5 June 2012, Accepted 6 September 2012, Scheduled 5 October 2012

* Corresponding author: Qaisar Abbas Naqvi (nqaisar@yahoo.com).

in such cases eases to solve [1] such problems. Shchukin [2] and Leontovich [3] introduced the idea of SIBC in 1940s [4]. Lindell and Sihvola [5] proposed the possible realization of such artificial surfaces which obey SIBC. In impedance boundary condition, the tangential components of electric and magnetic field are related through a relation

$$\mathbf{E} - (\hat{\mathbf{n}}.\mathbf{E})\hat{\mathbf{n}} = Z_s \hat{\mathbf{n}} \times \mathbf{H}$$

where the Z_s is the impedance of surface and $\hat{n}$ the unit normal to the surface.

A variety of methods have been applied to investigate the disk problem [6–34]. In most of the earlier work, disk is taken perfectly conducting and plane wave as source of excitation. However, Inawashiro [22] and Hongo et al. [23] have excited the perfectly conducting disk with dipole field. Jafri et al. [24] studied the scattering of impedance disk using KP method and Sebak and Shafai [25] investigated the arbitrarily shaped objects particulary impedance sphere and finite circular cylinder developing the integral equation and then applying the method of moments (MoM) [28] but both used the plane wave as source of excitation. In this paper, we have investigated the scattering of the field produced by an arbitrarily oriented dipole from circular disk with surface impedance first time by applying the KP method. This study is actually the extension of the work by Jafri et al. [24]. The KP method [29, 30] was initially developed to solve the potential problems associated with perfectly conducting disk and strip, but later successfully applied to perfectly conducting circular disk and circular disk with surface impedance [20–24] for time harmonic field.

The formulation of the problem starts with the defining the longitudinal components of the vector potentials of electric and magnetic types to express the scattered field in the form of Fourier-Hankel transform. The imposition of the required boundary conditions yields the dual integral equations (DIE). The equations may be written in the form of the vector Hankel transform given by Chew and Kong [31]. The DIEs solution is expanded in terms of a set of the functions with expansion coefficients. These functions are constructed by keeping in view the discontinuous properties of the Weber-Schafheitlin's integrals [35–37] and it is readily shown that these functions satisfy the required edge conditions [38–40] as well as boundary conditions. At this stage, we apply the projection using Jacobi polynomials as basis of the functional space. Thus the problem is reduced to the matrix equations for the expansion coefficient. The matrix equations are solved to determine the expansion coefficients. Numerical results for the far field patterns are obtained and compared with those obtained through physical optics method. The comparison shows that results match fairly well.

2. EXPRESSIONS FOR INCIDENT WAVE

The geometry of the problem under investigation is shown in Fig. 1. The dipole is located at (ρ_0, ϕ_0, z_0) and "a" is the radius of the disk. (ρ, ϕ, z) are the coordinates of the observation point. The electromagnetic field due to the dipole is derived in [23] and [41] and we just write the tangential components of the electromagnetic field for the disk problem.

$$\begin{pmatrix} \mathbf{E}^i \\ \mathbf{H}^i \end{pmatrix} = \sum_{m=0}^{\infty} \left\{ \mathbf{i}_\rho \left[\begin{pmatrix} E^i_{\rho c,m} \\ H^i_{\rho c,m} \end{pmatrix} \cos m\phi + \begin{pmatrix} E^i_{\rho s,m} \\ H^i_{\rho s,m} \end{pmatrix} \sin m\phi \right] + \mathbf{i}_\phi \left[\begin{pmatrix} E^i_{\phi c,m} \\ H^i_{\phi c,m} \end{pmatrix} \cos m\phi + \begin{pmatrix} E^i_{\phi s,m} \\ H^i_{\phi s,m} \end{pmatrix} \sin m\phi \right] \right\} \tag{1}$$

The expressions for the Fourier components defined in (1) at $z = 0$ are given as follows.

2.1. ρ-directed Dipole Field

$$E^i_{\rho c,m} = -\frac{1}{2\pi\kappa a^2} \int_0^\infty \frac{\exp(-jh_a z_{0a})}{\sqrt{\kappa^2 - \alpha^2}} \left[h_a^2 J'_m(\alpha\rho_{0a}) J'_m(\alpha\rho_a) + \kappa^2 \frac{m}{\alpha\rho_{0a}} J_m(\alpha\rho_{0a}) \frac{m}{\alpha\rho_a} J_m(\alpha\rho_a) \right] \alpha d\alpha \tag{2a}$$

$$E^i_{\phi s,m} = \frac{1}{2\pi\kappa a^2} \int_0^\infty \frac{\exp(-jh_a z_{0a})}{\sqrt{\kappa^2 - \alpha^2}} \left[h_a^2 J'_m(\alpha\rho_{0a}) \frac{m}{\alpha\rho_a} J_m(\alpha\rho_a) + \kappa^2 \frac{m}{\alpha\rho_{0a}} J_m(\alpha\rho_{0a}) J'_m(\alpha\rho_a) \right] \alpha d\alpha \tag{2b}$$

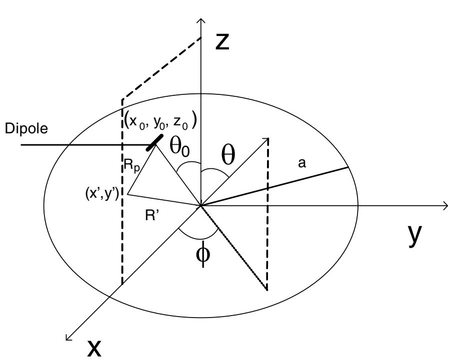

Figure 1. Scattering of an arbitrarily oriented dipole field by a circular disk with surface impedance.

$$H^i_{\rho s,m} = -\frac{Y_0}{2\pi a^2}\int_0^\infty \left[J'_m(\alpha\rho_a)\frac{m}{\alpha\rho_{0a}}J_m(\alpha\rho_{0a})+\frac{m}{\alpha\rho_a}J_m(\alpha\rho_a)J'_m(\alpha\rho_{0a})\right]$$
$$\exp(-jh_a z_{0a})\alpha d\alpha \tag{2c}$$

$$H^i_{\phi c,m} = \frac{Y_0}{2\pi a^2}\int_0^\infty \left[\frac{m}{\alpha\rho_a}J_m(\alpha\rho_a)\frac{m}{\alpha\rho_{0a}}J_m(\alpha\rho_{0a})+J'_m(\alpha\rho_a)J'_m(\alpha\rho_{0a})\right]$$
$$\exp(-jh_a z_{0a})\alpha d\alpha \tag{2d}$$

2.2. ϕ-directed Dipole Field

$$E^i_{\rho s,m} = -\frac{1}{2\pi\kappa a^2}\int_0^\infty \frac{\exp(-jh_a z_{0a})}{\sqrt{\kappa^2-\alpha^2}}$$
$$\left[h_a^2\frac{m}{\alpha\rho_{0a}}J_m(\alpha\rho_{0a})J'_m(\alpha\rho_a)+\kappa^2 J'_m(\alpha\rho_{0a})\frac{m}{\alpha\rho_a}J_m(\alpha\rho_a)\right]\alpha d\alpha \tag{3a}$$

$$E^i_{\phi c,m} = -\frac{1}{2\pi\kappa a^2}\int_0^\infty \frac{\exp(-jh_a z_{0a})}{\sqrt{\kappa^2-\alpha^2}}$$
$$\left[\kappa^2 J'_m(\alpha\rho_{0a})J'_m(\alpha\rho_a)+h_a^2\frac{m}{\alpha\rho_{0a}}J_m(\alpha\rho_{0a})\frac{m}{\alpha\rho_a}J_m(\alpha\rho_a)\right]\alpha d\alpha \tag{3b}$$

$$H^i_{\rho c,m} = -\frac{Y_0}{2\pi a^2}\int_0^\infty \left[J'_m(\alpha\rho_a)J'_m(\alpha\rho_{0a}) + \frac{m}{\alpha\rho_a}J_m(\alpha\rho_a)\frac{m}{\alpha\rho_{0a}}J_m(\alpha\rho_{0a})\right]$$
$$\exp(-jh_a z_{0a})\alpha d\alpha \tag{4a}$$

$$H^i_{\phi s,m} = \frac{Y_0}{2\pi a^2}\int_0^\infty \left[\frac{m}{\alpha\rho_a}J_m(\alpha\rho_a)J'_m(\alpha\rho_{0a}) + \frac{m}{\alpha\rho_{0a}}J_m(\alpha\rho_{0a})J'_m(\alpha\rho_a)\right]$$
$$\exp(-jh_a z_{0a})\alpha d\alpha \tag{4b}$$

2.3. z-directed Dipole Field

$$E^i_{\rho c,m} = \frac{1}{2\pi j\kappa a^2}\int_0^\infty J_m(\alpha\rho_{0a})J'_m(\alpha\rho_a)\exp(-jh_a z_{0a})\alpha^2 d\alpha \tag{5a}$$

$$E^i_{\phi s,m} = -\frac{1}{2\pi j\kappa a^2}\int_0^\infty J_m(\alpha\rho_{0a})\frac{m}{\alpha\rho_a}J_m(\alpha\rho_a)\exp(-jh_a z_{0a})\alpha^2 d\alpha \tag{5b}$$

$$H^i_{\rho s,m}=\frac{Y_0}{2\pi ja^2}\int_0^\infty \frac{1}{\sqrt{\kappa^2-\alpha^2}}J_m(\alpha\rho_{0a})\frac{m}{\alpha\rho_a}J_m(\alpha\rho_a)\exp(-jh_a z_{0a})\alpha^2 d\alpha \tag{6a}$$

$$H^i_{\phi c,m}=\frac{Y_0}{2\pi ja^2}\int_0^\infty \frac{1}{\sqrt{\kappa^2-\alpha^2}}J_m(\alpha\rho_{0a})J'_m(\alpha\rho_a)\exp(-jh_a z_{0a})\alpha^2 d\alpha \tag{6b}$$

where the variables and parameters used are normalized by the radius of the disk as

$$\rho_a = \frac{\rho}{a},\quad \rho_{0a} = \frac{\rho_0}{a},\quad z_a = \frac{z}{a},\quad z_{0a} = \frac{z_0}{a},$$
$$h_a = ha,\quad \kappa = ka,\quad h = \sqrt{\kappa^2-\alpha^2}$$

$Y_0 = \sqrt{\frac{\epsilon_0}{\mu_0}}$ is the intrinsic admittance of free space and k the wave number. $J_m(x)$ and $J'_m(x)$ are the Bessel function of the first kind and its derivative with respect to the argument.

3. THE EXPRESSIONS FOR SCATTERED FIELD

Here we discuss how the KP method is applied for predicting the field scattered by an impedance disk.

3.1. Spectrum Functions of the Fields on the Disk

The magnetic and electric vector potential corresponding to the scattered field are defined in terms of unknown weighting functions $\widetilde{f}(\xi)$ and $\widetilde{g}(\xi)$ which are to be determined so that they satisfy the required boundary conditions.

$$\begin{aligned} A_z^{s\pm}(\rho,\phi,z) = {} & \mu_0 a\kappa Y_0 \sum_{m=0}^{\infty}\int_0^{\infty}\left[\widetilde{f}_{cm}^{\pm}(\xi)\cos m\phi+\widetilde{f}_{sm}^{\pm}(\xi)\sin m\phi\right] \\ & J_m(\rho_a\xi)\exp[\mp\sqrt{\xi^2-\kappa^2}\,z_a]\xi^{-1}d\xi \qquad \text{(7a)} \\ F_z^{s\pm}(\rho,\phi,z) = {} & \epsilon_0 a \sum_{m=0}^{\infty}\int_0^{\infty}\left[\widetilde{g}_{cm}^{\pm}(\xi)\cos m\phi+\widetilde{g}_{sm}^{\pm}(\xi)\sin m\phi\right] \\ & J_m(\rho_a\xi)\exp[\mp\sqrt{\xi^2-\kappa^2}\,z_a]\xi^{-1}d\xi \qquad \text{(7b)} \end{aligned}$$

where the upper and lower signs refer to the region $z > 0$ and $z < 0$, respectively.

The boundary conditions for this problem are stated as

(1) The tangential components of electric and magnetic fields are continuous on the plane $z = 0$ for $\rho_a \geq 1$.

(2) $E_\rho^+ = -Z_s^+ H_\phi^+$, $E_\rho^- = Z_s^- H_\phi^-$, $E_\phi^+ = Z_s^+ H_\rho^+$, $E_\phi^- = -Z_s^- H_\rho^-$ for $\rho_a \leq 1$ where Z_s^+ and Z_s^- are assumed to be surface impedances of upper and lower surfaces respectively.

The first boundary condition gives

$$\begin{aligned} & \begin{bmatrix} E_{\rho c,m}^{s+}(\rho_a) - E_{\rho c,m}^{s-}(\rho_a) \\ E_{\phi s,m}^{s+}(\rho_a) - E_{\phi s,m}^{s-}(\rho_a) \end{bmatrix} \\ & = \int_0^{\infty}\left[H^-(\xi\rho_a)\right]\begin{bmatrix} j\sqrt{\xi^2-\kappa^2}\left[\widetilde{f}_{cm}^{+}(\xi)+\widetilde{f}_{cm}^{-}(\xi)\right]\xi^{-1} \\ \left[\widetilde{g}_{sm}^{+}(\xi)-\widetilde{g}_{sm}^{-}(\xi)\right]\xi^{-1} \end{bmatrix}\xi d\xi = 0 \\ & = \int_0^{\infty}\left[H^-(\xi\rho_a)\right]\begin{bmatrix} \widetilde{E}_{\rho c,m}(\xi) \\ \widetilde{E}_{\phi s,m}(\xi) \end{bmatrix}\xi d\xi = 0, \qquad \rho_a \geq 1 \qquad \text{(8a)} \end{aligned}$$

$$\begin{aligned}
&\begin{bmatrix} E^{s+}_{\rho s,m}(\rho_a) - E^{s-}_{\rho s,m}(\rho_a) \\ E^{s+}_{\phi c,m}(\rho_a) - E^{s-}_{\phi c,m}(\rho_a) \end{bmatrix} \\
&= \int_0^\infty \left[H^+(\xi\rho_a)\right] \begin{bmatrix} j\sqrt{\xi^2-\kappa^2}\left[\widetilde{f}^+_{sm}(\xi) + \widetilde{f}^-_{sm}(\xi)\right]\xi^{-1} \\ \left[\widetilde{g}^+_{cm}(\xi) - \widetilde{g}^-_{cm}(\xi)\right]\xi^{-1} \end{bmatrix} \xi d\xi = 0 \\
&= \int_0^\infty \left[H^+(\xi\rho_a)\right] \begin{bmatrix} \widetilde{E}_{\rho s,m}(\xi) \\ \widetilde{E}_{\phi c,m}(\xi) \end{bmatrix} \xi d\xi = 0, \qquad \rho_a \geq 1 \qquad \text{(8b)} \\
&\begin{bmatrix} H^{s+}_{\rho c,m}(\rho_a) - H^{s-}_{\rho c,m}(\rho_a) \\ H^{s+}_{\phi s,m}(\rho_a) - H^{s-}_{\phi s,m}(\rho_a) \end{bmatrix} \\
&= Y_0 \int_0^\infty \left[H^-(\xi\rho_a)\right] \begin{bmatrix} j\sqrt{\xi^2-\kappa^2}\left[\widetilde{g}^+_{cm}(\xi) + \widetilde{g}^-_{cm}(\xi)\right](\kappa\xi)^{-1} \\ -\kappa\left[\widetilde{f}^+_{sm}(\xi) - \widetilde{f}^-_{sm}(\xi)\right]\xi^{-1} \end{bmatrix} \xi d\xi = 0 \\
&= \int_0^\infty \left[H^-(\xi\rho_a)\right] \begin{bmatrix} \widetilde{H}_{\rho c,m}(\xi) \\ \widetilde{H}_{\phi s,m}(\xi) \end{bmatrix} \xi d\xi = 0, \qquad \rho_a \geq 1 \qquad \text{(8c)} \\
&\begin{bmatrix} H^{s+}_{\rho s,m}(\rho_a) - H^{s-}_{\rho s,m}(\rho_a) \\ H^{s+}_{\phi c,m}(\rho_a) - H^{s-}_{\phi c,m}(\rho_a) \end{bmatrix} \\
&= Y_0 \int_0^\infty \left[H^+(\xi\rho_a)\right] \begin{bmatrix} j\sqrt{\xi^2-\kappa^2}\left[\widetilde{g}^+_{sm}(\xi) + \widetilde{g}^-_{sm}(\xi)\right](\kappa\xi^{)}-1 \\ -\kappa\left[\widetilde{f}^+_{cm}(\xi) - \widetilde{f}^-_{cm}(\xi)\right]\xi^{-1} \end{bmatrix} \xi d\xi = 0 \\
&= \int_0^\infty \left[H^+(\xi\rho_a)\right] \begin{bmatrix} \widetilde{H}_{\rho s,m}(\xi) \\ \widetilde{H}_{\phi c,m}(\xi) \end{bmatrix} \xi d\xi = 0, \qquad \rho_a \geq 1 \qquad \text{(8d)}
\end{aligned}$$

where the kernel matrices $[H^+(\xi\rho_a)]$ and $[H^-(\xi\rho_a)]$ are given by

$$\left[H^\pm(\xi\rho_a)\right] = \begin{bmatrix} J'_m(\xi\rho_a) & \pm\frac{m}{\xi\rho_a}J_m(\xi\rho_a) \\ \pm\frac{m}{\xi\rho_a}J_m(\xi\rho_a) & J'_m(\xi\rho_a) \end{bmatrix} \tag{9}$$

Equation (8) is one set of DIEs, and the solution of these equations must satisfy the Maxwell equations and edge conditions. The solution of these DIEs is expanded in terms of such functions with expansion coefficients by taking into account the discontinuous properties of the Weber-Schafheitlin's integrals and then unknown weighting functions are derived in terms of these functions. This has been done in [24] and we are here just writing the result.

$$\begin{aligned}
\widetilde{f}^\pm_{cm}(\xi) = \frac{1}{2}\Bigg[&\frac{1}{j\sqrt{\xi^2-\kappa^2}}\sum_{n=0}^\infty \left[A^E_{mn}\Xi^-_{mn}(\xi) - B^E_{mn}\Gamma^+_{mn}(\xi)\right] \\
&\mp\frac{Z_0}{\kappa}\sum_{n=0}^\infty \left[C^H_{mn}\Xi^+_{mn}(\xi) + D^H_{mn}\Gamma^-_{mn}(\xi)\right]\Bigg]\xi \qquad \text{(10a)}
\end{aligned}$$

$$\widetilde{f}_{sm}^{\pm}(\xi) = \frac{1}{2}\left[\frac{1}{j\sqrt{\xi^2-\kappa^2}}\sum_{n=0}^{\infty}\left[C_{mn}^{E}\Xi_{mn}^{-}(\xi)+D_{mn}^{E}\Gamma_{mn}^{+}(\xi)\right]\right.$$
$$\left.\mp\frac{Z_0}{\kappa}\sum_{n=0}^{\infty}\left[-A_{mn}^{H}\Xi_{mn}^{+}(\xi)+B_{mn}^{H}\Gamma_{mn}^{-}(\xi)\right]\right]\xi \qquad (10b)$$

$$\widetilde{g}_{cm}^{\pm}(\xi) = \frac{1}{2}\left[\frac{\kappa Z_0}{j\sqrt{\xi^2-\kappa^2}}\sum_{n=0}^{\infty}\left[A_{mn}^{H}\Xi_{mn}^{-}(\xi)-B_{mn}^{H}\Gamma_{mn}^{+}(\xi)\right]\right.$$
$$\left.\pm\sum_{n=0}^{\infty}\left[C_{mn}^{E}\Xi_{mn}^{+}(\xi)+D_{mn}^{E}\Gamma_{mn}^{-}(\xi)\right]\right]\xi \qquad (10c)$$

$$\widetilde{g}_{sm}^{\pm}(\xi) = \frac{1}{2}\left[\frac{\kappa Z_0}{j\sqrt{\xi^2-\kappa^2}}\sum_{n=0}^{\infty}\left[C_{mn}^{H}\Xi_{mn}^{-}(\xi)+D_{mn}^{H}\Gamma_{mn}^{+}(\xi)\right]\right.$$
$$\left.\pm\sum_{n=0}^{\infty}\left[-A_{mn}^{E}\Xi_{mn}^{+}(\xi)+B_{mn}^{H}\Gamma_{mn}^{-}(\xi)\right]\right]\xi \qquad (10d)$$

In the above equations the functions $\Xi_{mn}^{\pm}(\xi)$ and $\Gamma_{mn}^{\pm}(\xi)$ are defined as

$$\Xi_{mn}^{\pm}(\xi) = \left[J_{m+2n}(\xi)\pm J_{m+2n+2}(\xi)\right]\xi^{-1},$$
$$\Gamma_{mn}^{\pm}(\xi) = \left[J_{m+2n+1}(\xi)\pm J_{m+2n+3}(\xi)\right]\xi^{-2}$$

and $A_{mn}^{E,H} \sim D_{mn}^{E,H}$ are expansion coefficients.

The second boundary condition yields

$$\begin{bmatrix}E_{\rho c,m}^{t+}(\rho_a)\\ E_{\phi s,m}^{t+}(\rho_a)\end{bmatrix} = \mp Z_s^{+}\begin{bmatrix}H_{\phi c,m}^{t+}(\rho_a)\\ H_{\rho s,m}^{t+}(\rho_a)\end{bmatrix}=0,$$
$$\begin{bmatrix}E_{\rho s,m}^{t+}(\rho_a)\\ E_{\phi c,m}^{t+}(\rho_a)\end{bmatrix} = \mp Z_s^{+}\begin{bmatrix}H_{\phi s,m}^{t+}(\rho_a)\\ H_{\rho c,m}^{t+}(\rho_a)\end{bmatrix}=0, \quad \rho_a\le 1 \qquad (11a)$$

$$\begin{bmatrix}E_{\rho c,m}^{t-}(\rho_a)\\ E_{\phi s,m}^{t-}(\rho_a)\end{bmatrix} = \pm Z_s^{-}\begin{bmatrix}H_{\phi c,m}^{t-}(\rho_a)\\ H_{\rho s,m}^{t-}(\rho_a)\end{bmatrix}=0,$$
$$\begin{bmatrix}E_{\rho s,m}^{t-}(\rho_a)\\ E_{\phi c,m}^{t-}(\rho_a)\end{bmatrix} = \pm Z_s^{-}\begin{bmatrix}H_{\phi s,m}^{t-}(\rho_a)\\ H_{\rho c,m}^{t-}(\rho_a)\end{bmatrix}=0, \quad \rho_a\le 1 \qquad (11b)$$

where

$$\begin{bmatrix}H_{\rho c,m}^{t\pm}(\rho_a)\\ H_{\phi s,m}^{t\pm}(\rho_a)\end{bmatrix} = \begin{bmatrix}H_{\rho c,m}^{s\pm}(\rho_a)\\ H_{\phi s,m}^{s\pm}(\rho_a)\end{bmatrix}+\begin{bmatrix}H_{\rho c,m}^{i}(\rho_a)\\ H_{\phi s,m}^{i}(\rho_a)\end{bmatrix},$$
$$\begin{bmatrix}H_{\rho s,m}^{t\pm}(\rho_a)\\ H_{\phi c,m}^{t\pm}(\rho_a)\end{bmatrix} = \begin{bmatrix}H_{\rho s,m}^{s\pm}(\rho_a)\\ H_{\phi c,m}^{s\pm}(\rho_a)\end{bmatrix}+\begin{bmatrix}H_{\rho s,m}^{i}(\rho_a)\\ H_{\phi c,m}^{i}(\rho_a)\end{bmatrix} \qquad (11c)$$

$$\begin{bmatrix} E^{t\pm}_{\rho c,m}(\rho_a) \\ E^{t\pm}_{\phi s,m}(\rho_a) \end{bmatrix} = \begin{bmatrix} E^{s\pm}_{\rho c,m}(\rho_a) \\ E^{s\pm}_{\phi s,m}(\rho_a) \end{bmatrix} + \begin{bmatrix} E^{i}_{\rho c,m}(\rho_a) \\ E^{i}_{\phi s,m}(\rho_a) \end{bmatrix},$$
$$\begin{bmatrix} E^{t\pm}_{\rho s,m}(\rho_a) \\ E^{t\pm}_{\phi c,m}(\rho_a) \end{bmatrix} = \begin{bmatrix} E^{s\pm}_{\rho s,m}(\rho_a) \\ E^{s\pm}_{\phi c,m}(\rho_a) \end{bmatrix} + \begin{bmatrix} E^{i}_{\rho s,m}(\rho_a) \\ E^{i}_{\phi c,m}(\rho_a) \end{bmatrix} \tag{11d}$$

3.2. Derivation of the Expansion Coefficients

In the Equation (11), we substitute the $E^{s\pm}, E^i$ and $H^{s\pm}, H^i$ and project the resulting equations into the functional space with elements P_n^m.

$$x^{-m/2} J_m(\xi\sqrt{x}) = \sum_{n=0}^{\infty} 2(m+2n+1)\frac{\Gamma(m+n+1)}{\Gamma(m+1)\Gamma(n+1)}\frac{J_{m+2n+1}(\xi)}{\xi}P_n^m$$
$$P_n^m = \frac{\Gamma(m+1)\Gamma(n+1)}{\Gamma(m+n+1)}x^{-m/2}\int_0^{\infty} J_m(\xi\sqrt{x})J_{m+2n+1}(\xi)d\xi$$

The normalized surface impedances of upper and lower surfaces are taken equal, i.e., $\zeta_{\pm} = \frac{Z_s^{\pm}}{Z_0} = \zeta$, so that the resulting equations are simplified. After some manipulation, these equations reduce to matrix equations of expansion coefficients. The matrix equations for expansion coefficients $(A^E_{mn}, B^E_{mn}, C^H_{mn}, D^H_{mn})$ are

$$\sum_{n=0}^{\infty}\left[A^E_{mn}Z^{(1,1)}_{mp,n} - B^E_{mn}Z^{(1,2)}_{mp,n}\right] = H^{(1)}_{m,p},$$
$$\sum_{n=0}^{\infty}\left[-A^E_{mn}Z^{(2,1)}_{mp,n} + B^E_{mn}Z^{(2,2)}_{mp,n}\right] = H^{(2)}_{m,p}, \tag{12a}$$

$$\sum_{n=0}^{\infty}\left[C^H_{mn}Z'^{(1,1)}_{mp,n} + D^H_{mn}Z'^{(1,2)}_{mp,n}\right] = H'^{(1)}_{m,p},$$
$$\sum_{n=0}^{\infty}\left[C^H_{mn}Z'^{(2,1)}_{mp,n} + D^H_{mn}Z'^{(2,2)}_{mp,n}\right] = H'^{(2)}_{m,p} \tag{12b}$$

$$\sum_{n=0}^{\infty} A^E_{0n}Z^{(1,1)}_{0p,n} = H^{(1)}_{0,p}, \qquad \sum_{n=0}^{\infty} D^H_{0n}Z'^{(1,2)}_{0p,n} = H'^{(1)}_{0,p} \tag{12c}$$
$$m = 1, 2, 3, \ldots; \quad p = 0, 1, 2, 3, \ldots;$$

The matrix equations for expansion coefficients $(A^H_{mn}, B^H_{mn}, C^E_{mn}, D^E_{mn})$ are

$$\begin{aligned}
&\sum_{n=0}^{\infty}\left[A^H_{mn}Z'^{(1,1)}_{mp,n} - B^H_{mn}Z'^{(1,2)}_{mp,n}\right] = K'^{(1)}_{m,p},\\
&\sum_{n=0}^{\infty}\left[A^H_{mn}Z^{('2,1)}_{mp,n} - B^H_{mn}Z'^{(2,2)}_{mp,n}\right] = K'^{(2)}_{m,p},
\end{aligned} \tag{13a}$$

$$\begin{aligned}
&\sum_{n=0}^{\infty}\left[C^E_{mn}Z^{(1,1)}_{mp,n} + D^E_{mn}Z^{(1,2)}_{mp,n}\right] = K^{(1)}_{m,p},\\
&\sum_{n=0}^{\infty}\left[C^E_{mn}Z^{(2,1)}_{mp,n} + D^E_{mn}Z^{(2,2)}_{mp,n}\right] = K^{(2)}_{m,p}
\end{aligned} \tag{13b}$$

$$\sum_{n=0}^{\infty}A^H_{0n}Z'^{(1,1)}_{0p,n} = K'^{(2)}_{0,p}, \qquad \sum_{n=0}^{\infty}D^E_{0n}Z^{(1,2)}_{0p,n} = K^{(2)}_{0,p} \tag{13c}$$

$$m = 1, 2, 3, \ldots; \qquad p = 0, 1, 2, 3, \ldots$$

and $H_{m,p} \sim H'_{m,p}$ and $K_{m,p} \sim K'_{m,p}$ are defined below. The elements $Z^{(1,1)}_{mp,n} \sim Z^{(2,2)}_{mp,n}$ and $Z'^{(1,1)}_{mp,n} \sim Z'^{(2,2)}_{mp,n}$ of the Equations (12) and (13) are same as in [24], so we are skipping their definitions.

3.2.1. ρ-directed Dipole

$$H^{(1)}_{m,p}=\frac{\zeta}{2\pi a^2}\int_0^{\infty}\Bigg[2m\left(\alpha^m_p+1\right)J_{m+2p+1}(\xi)\xi^{-2}\frac{m}{\xi\rho_{0a}}J_m(\xi\rho_{0a}) \\ +(\alpha^m_p J_{m+2p}(\xi)-(\alpha^m_p+2)J_{m+2p+2}(\xi))\xi^{-1}J'_m(\xi\rho_{0a})\Bigg]\exp(-jh_a z_{0a})\xi d\xi \tag{14a}$$

$$H^{(2)}_{m,p}=\frac{\zeta}{2\pi a^2}\int_0^{\infty}\Bigg[\left(\alpha^m_p J_{m+2p}(\xi)-(\alpha^m_p+2)J_{m+2p+2}(\xi)\right)\xi^{-1}\frac{m}{\xi\rho_{0a}}J_m(\xi\rho_{0a}) \\ +2m(\alpha^m_p+1)J_{m+2p+1}(\xi)\xi^{-2}J'_m(\xi\rho_{0a})\Bigg]\exp(-jh_a z_{0a})\xi d\xi \tag{14b}$$

$$H'^{(1)}_{m,p}=-\frac{1}{2\pi\kappa a^2}\int_0^\infty \exp(-jh_a z_{0a}) \left[\sqrt{\kappa^2-\xi^2}J'_m(\xi\rho_{0a})(\alpha_p^m J_{m+2p}(\xi)-(\alpha_p^m+2)J_{m+2p+2}(\xi))\xi^{-1} +\kappa^2\frac{m}{\xi\rho_{0a}\sqrt{\kappa^2-\xi^2}}J_m(\xi\rho_{0a})2m(\alpha_p^m+1)J_{m+2p+1}(\xi)\xi^{-2}\right]\xi d\xi \tag{14c}$$

$$H'^{(2)}_{m,p}=-\frac{1}{2\pi\kappa a^2}\int_0^\infty \exp(-jh_a z_{0a})\left[\sqrt{\kappa^2-\xi^2}J'_m(\xi\rho_{0a})2m(\alpha_p^m+1) J_{m+2p+1}(\xi)\xi^{-2}+\kappa^2\frac{m}{\xi\rho_{0a}\sqrt{\kappa^2-\xi^2}}J_m(\xi\rho_{0a})(\alpha_p^m J_{m+2p}(\xi) -(\alpha_p^m+2)J_{m+2p+2}(\xi))\xi^{-1}\right]\xi d\xi \tag{14d}$$

3.2.2. ϕ-directed Dipole

$$K^{(1)}_{m,p}=\frac{1}{2\pi\kappa a^2}\int_0^\infty \exp(-jh_a z_{0a})\left[\sqrt{\kappa^2-\alpha^2} \frac{m}{\alpha\rho_{0a}}J_m(\alpha\rho_{0a})(\alpha_p^m J_{m+2p}(\alpha)-(\alpha_p^m+2)J_{m+2p+2}(\alpha))\alpha^{-1} +\frac{\kappa^2}{\sqrt{\kappa^2-\alpha^2}}J'_m(\alpha\rho_{0a})2m(\alpha_p^m+1)J_{m+2p+1}(\alpha)\alpha^{-2}\right]\alpha d\alpha \tag{15a}$$

$$K^{(2)}_{m,p}=\frac{1}{2\pi\kappa a^2}\int_0^\infty \exp(-jh_a z_{0a})\left[\frac{\kappa^2}{\sqrt{\kappa^2-\alpha^2}} J'_m(\alpha\rho_{0a})(\alpha_p^m J_{m+2p}(\alpha)-(\alpha_p^m+2)J_{m+2p+2}(\alpha))\alpha^{-1} +\sqrt{\kappa^2-\alpha^2}\frac{m}{\alpha\rho_{0a}}J_m(\alpha\rho_{0a})2m(\alpha_p^m+1)J_{m+2p+1}(\alpha)\alpha^{-2}\right]\alpha d\alpha \tag{15b}$$

$$K'^{(1)}_{m,p}=\frac{\zeta}{2\pi a^2}\int_0^\infty\left[J'_m(\alpha\rho_{0a})2m(\alpha_p^m+1)J_{m+2p+1}(\alpha)\alpha^{-2} +\frac{m}{\alpha\rho_{0a}}J_m(\alpha\rho_{0a})(\alpha_p^m J_{m+2p}(\alpha)-(\alpha_p^m+2)J_{m+2p+2}(\alpha))\alpha^{-1}\right] \exp(-jh_a z_{0a})\alpha d\alpha \tag{15c}$$

$$K'^{(2)}_{m,p} = \frac{\zeta}{2\pi a^2}\int_0^\infty \left[J'_m(\alpha\rho_{0a})(\alpha_p^m J_{m+2p}(\alpha) - (\alpha_p^m + 2)J_{m+2p+2}(\alpha))\alpha^{-1} + \frac{m}{\alpha\rho_{0a}} J_m(\alpha\rho_{0a})2m(\alpha_p^m + 1)J_{m+2p+1}(\alpha)\alpha^{-2}\right] \exp(-jh_a z_{0a})\alpha d\alpha \tag{15d}$$

3.2.3. z-directed Dipole

$$H^{(1)}_{m,p} = -\frac{j}{2\pi a^2}\int_0^\infty \frac{1}{\sqrt{\kappa^2-\alpha^2}} J_m(\alpha\rho_{0a})(\alpha_p^m J_{m+2p}(\alpha) - (\alpha_p^m+2)J_{m+2p+2}(\alpha))\alpha^{-1}\exp(-jh_a z_{0a})\alpha^2 d\alpha \tag{16a}$$

$$H^{(2)}_{m,p} = \frac{j}{2\pi a^2}\int_0^\infty \frac{1}{\sqrt{\kappa^2-\alpha^2}} J_m(\alpha\rho_{0a}) 2m(\alpha_p^m + 1)J_{m+2p+1}(\alpha)\alpha^{-2}\exp(-jh_a z_{0a})\alpha^2 d\alpha \tag{16b}$$

$$H'^{(1)}_{m,p} = -\frac{j\zeta}{2\pi\kappa a^2}\int_0^\infty J_m(\alpha\rho_{0a})(\alpha_p^m J_{m+2p}(\alpha) - (\alpha_p^m + 2)J_{m+2p+2}(\alpha))\alpha^{-1}\exp(-jh_a z_{0a})\alpha^2 d\alpha \tag{16c}$$

$$H'^{(2)}_{m,p} = -\frac{j\zeta}{2\pi\kappa a^2}\int_0^\infty J_m(\alpha\rho_{0a})2m (\alpha_p^m + 1)J_{m+2p+1}(\alpha)\alpha^{-2}\exp(-jh_a z_{0a})\alpha^2 d\alpha \tag{16d}$$

3.3. Far Field Expression

The far field expressions of A_z^s and F_z^s are obtained by applying the stationary phase method of integration. The expressions given in (7) can be written in the form

$$I_{nt} = \int_0^\infty \widetilde{P}(\xi)J_m(\rho_a\xi)\exp\left[-\sqrt{\xi^2-\kappa^2}\ z_a\right]\xi^{-1}d\xi$$

Application of the standard process of the method to the above integral gives the result in the form given by

$$I_{nt} = \exp\left(j\frac{m+1}{2}\pi\right)\frac{\exp(-jkR)}{kR}\widetilde{P}(\kappa\sin\theta)\frac{\cos\theta}{\sin\theta} \tag{17}$$

If we apply this formula to the vector potentials given in (7), we get

$$\begin{aligned} A_z^s(\mathbf{r}) \;=\; & \mu_0 a^2 Y_0 \frac{\exp(-jkR)}{kR}\frac{1}{\sin\theta} \\ & \Bigg\{ \sum_{n=0}^{\infty} j \left[A_{0n}^E \frac{J_{2n+2}(\kappa\sin\theta)}{(\kappa\sin\theta)} - Z_0\cos\theta D_{0n}^H \frac{J_{2n+3}(\kappa\sin\theta)}{(\kappa\sin\theta)^2} \right] \\ & -\frac{1}{2}\sum_{m=1}^{\infty} j^{m+1} \sum_{n=0}^{\infty} \Big\{ \left[A_{mn}^E \Xi_{mn}^-(\kappa\sin\theta) - B_{mn}^E \Gamma_{mn}^+(\kappa\sin\theta) \right] \\ & +Z_0\cos\theta \left[C_{mn}^H \Xi_{mn}^+(\kappa\sin\theta) + D_{mn}^H \Gamma_{mn}^-(\kappa\sin\theta) \right] \cos m\phi \\ & +Z_0\cos\theta \left[-A_{mn}^H \Xi_{mn}^+(\kappa\sin\theta) + B_{mn}^H \Gamma_{mn}^-(\kappa\sin\theta) \right] \\ & + \left[C_{mn}^E \Xi_{mn}^-(\kappa\sin\theta) + D_{mn}^E \Gamma_{mn}^+(\kappa\sin\theta) \right] \sin m\phi \Big\} \Bigg\} \end{aligned} \tag{18a}$$

$$\begin{aligned} F_z^s(\mathbf{r}) \;=\; & \epsilon_0 a \frac{\exp(-jkR)}{kR}\frac{1}{\sin\theta} \\ & \Bigg\{ \sum_{n=0}^{\infty} j \left[Z_0 A_{0n}^H \frac{J_{2n+2}(\kappa\sin\theta)}{(\kappa\sin\theta)} - \cos\theta D_{0n}^E \frac{J_{2n+3}(\kappa\sin\theta)}{(\kappa\sin\theta)^2} \right] \\ & -\frac{1}{2}\sum_{m=1}^{\infty} j^{m+1} \sum_{n=0}^{\infty} \Big\{ Z_0 \left[A_{mn}^H \Xi_{mn}^-(\kappa\sin\theta) - B_{mn}^H \Gamma_{mn}^+(\kappa\sin\theta) \right] \\ & -\cos\theta \left[C_{mn}^E \Xi_{mn}^+(\kappa\sin\theta) + D_{mn}^E \Gamma_{mn}^-(\kappa\sin\theta) \right] \cos m\phi \\ & +\cos\theta \left[A_{mn}^E \Xi_{mn}^+(\kappa\sin\theta) - B_{mn}^E \Gamma_{mn}^-(\kappa\sin\theta) \right] \\ & +Z_0 \left[C_{mn}^H \Xi_{mn}^-(\kappa\sin\theta) + D_{mn}^H \Gamma_{mn}^+(\kappa\sin\theta) \right] \sin m\phi \Big\} \Bigg\} \end{aligned} \tag{18b}$$

In the far region we have the relations

$$\begin{aligned} & E_\theta = -j\omega A_\theta = j\omega\sin\theta A_z, \\ & H_\theta = -j\omega F_\theta = j\omega\sin\theta F_z = -Y_0 E_\phi, \quad A_\phi = Z_0\sin\theta F_z \end{aligned} \tag{19}$$

3.4. Physical Optics Approximate Solutions

Here we derive the physical optics solutions in order to compare with the KP solutions. Since we assume the dipole is placed at $\phi_0 = 0$, so ρ- and ϕ-directed dipole can be treated as x- and y-directed dipole respectively.

3.4.1. x-directed Dipole

The incident and reflected field are

$$A_x^i = \frac{I_0}{4\pi}\frac{\exp(-jkR_p)}{R_p} \tag{20a}$$

$$\mathbf{H}^i = \frac{I_0}{4\pi}\left[\hat{y}z_0 + \hat{z}(y'-y_0)\right]\left[jk+\frac{1}{R_p}\right]\frac{\exp(-jkR_p)}{R_p^2} \tag{20b}$$

$$\mathbf{E}^i = -\frac{jkZ_0I_0}{4\pi}\left\{\frac{\hat{x}(x'-x_0)^2+\hat{y}(y'-y_0)(x'-x_0)-\hat{z}(z_0)(x'-x_0)}{R_p^2}\alpha+\hat{x}\beta\right\}\frac{\exp(-jkR_p)}{R_p} \tag{20c}$$

$$\mathbf{H}^r = A\frac{I_0}{4\pi}\left[-\hat{y}z_0 + \hat{z}(y'-y_0)\right]\left[jk+\frac{1}{R_p}\right]\frac{\exp(-jkR_p)}{R_p^2} \tag{20d}$$

$$\mathbf{E}^r = -A\frac{jkZ_0I_0}{4\pi}\left\{\frac{\hat{x}(x'-x_0)^2+\hat{y}(y'-y_0)(x'-x_0)+\hat{z}(z_0)(x'-x_0)}{R_p^2}\alpha+\hat{x}\beta\right\}\frac{\exp(-jkR_p)}{R_p} \tag{20e}$$

where I_0 is the strength of the dipole current, (x', y') the rectangular coordinates of a point on the circular disk, (θ, ϕ) the spherical angular coordinates of the observation point, R the distance of the observation point from the center of the disk, and R_p the distance between the source point and the point on the disk. R and R_p are given by

$$R = \sqrt{x^2+y^2+z^2}, \qquad R_p = \sqrt{(x'-x_0)^2+(y'-y_0)^2+z_0^2} \tag{20f}$$

In order to determine the current densities, we apply the SIBC on the plane $z = 0$ and get the reflection coefficient as $A = \frac{\zeta^+\gamma z_0-\alpha(x'-x_0)^2-\beta R_p^2}{\zeta^+\gamma z_0+\alpha(x'-x_0)^2+\beta R_p^2}$, where

$$\alpha = \frac{3}{k^2R_p^2}+\frac{3j}{kR_p}-1, \quad \beta = 1-\frac{1}{k^2R_p^2}-\frac{j}{kR_p}, \quad \gamma = R_p+\frac{-j}{k}$$

In case, surface impedance becomes zero this leads to the case of perfectly conducting disk as it should be giving the reflection coefficient -1.

The current densities are

$$\mathbf{M} = -\hat{n}\times\mathbf{E}^{tot}, \qquad \mathbf{J} = \hat{n}\times\mathbf{H}^{tot} \tag{21a}$$

$$\mathbf{M} = \frac{\zeta^+\gamma z_0}{\zeta^+\gamma z_0+\alpha(x'-x_0)^2+\beta R_p^2}\frac{jkZ_0I_0}{2\pi}$$

$$\left\{\frac{\hat{y}(x'-x_0)^2-\hat{x}(y'-y_0)(x'-x_0)}{R_p^2}\alpha+\hat{y}\beta\right\}\frac{\exp(-jkR_p)}{R_p} \tag{21b}$$

$$\mathbf{J}=\frac{(\alpha(x'-x_0)^2+\beta R_p^2)}{\zeta^+\gamma z_0+\alpha(x'-x_0)^2+\beta R_p^2}\frac{I_0}{2\pi}\left[-\hat{x}z_0\right]\left[jk+\frac{1}{R_p}\right]\frac{\exp(-jkR_p)}{R_p^2} \tag{21c}$$

The corresponding vector potentials are

$$A_x=-\frac{\mu I_0}{8\pi^2 R}\exp(-jkR)\int_S\frac{(\alpha(x'-x_0)^2+\beta R_p^2)}{\zeta^+\gamma z_0+\alpha(x'-x_0)^2+\beta R_p^2}\left[jk+\frac{1}{R_p}\right]$$

$$\frac{z_0}{R_p^2}\exp(-jkR_p)\times\exp\left[jk\sin\theta(x'\cos\phi+y'\sin\phi)\right]dx'dy' \tag{22a}$$

$$F_x=-\frac{\mu I_0}{8\pi^2 R}\exp(-jkR)$$

$$\int_S\frac{\zeta^+\gamma z_0}{\zeta^+\gamma z_0+\alpha(x'-x_0)^2+\beta R_p^2}\alpha\frac{(y'-y_0)(x'-x_0)}{R_p^3}\exp(-jkR_p)$$

$$\times\exp\left[jk\sin\theta(x'\cos\phi+y'\sin\phi)\right]dx'dy' \tag{22b}$$

$$F_y=\frac{\mu I_0}{8\pi^2 R}\exp(-jkR)\int_S\frac{\zeta^+\gamma z_0}{\zeta^+\gamma z_0+\alpha(x'-x_0)^2+\beta R_p^2}\left(\frac{\alpha(x'-x_0)^2}{R_p^2}+\beta\right)$$

$$\frac{\exp(-jkR_p)}{R_p}\times\exp\left[jk\sin\theta(x'\cos\phi+y'\sin\phi)\right]dx'dy' \tag{22c}$$

3.4.2. y-directed Dipole

The incident vector potential is

$$A_y^i=\frac{I_0}{4\pi}\frac{\exp(-jkR_p)}{R_p} \tag{23}$$

We obtain the current densities and corresponding vector potentials in similar way as in x-directed case. The current densities are

$$\mathbf{M}=\frac{\zeta^+\gamma z_0}{\zeta^+\gamma z_0+\alpha(y'-y_0)^2+\beta R_p^2}\frac{jkZ_0 I_0}{2\pi}$$

$$\left\{\frac{\hat{y}(x'-x_0)(y'-y_0)-\hat{x}(y'-y_0)^2}{R_p^2}\alpha-\hat{x}\beta\right\}\frac{\exp(-jkR_p)}{R_p} \tag{24a}$$

$$\mathbf{J}=\frac{(\alpha(y'-y_0)^2+\beta R_p^2)}{\zeta^+\gamma z_0+\alpha(y'-y_0)^2+\beta R_p^2}\frac{I_0}{2\pi}\left[-\hat{x}z_0\right]\left[jk+\frac{1}{R_p}\right]\frac{\exp(-jkR_p)}{R_p^2} \tag{24b}$$

The corresponding vector potentials are

$$A_y = -\frac{\mu I_0}{8\pi^2 R}\exp(-jkR)\int_S \frac{\left(\alpha(y'-y_0)^2+\beta R_p^2\right)}{\zeta^+\gamma z_0+\alpha(y'-y_0)^2+\beta R_p^2}\left[jk+\frac{1}{R_p}\right]dy'$$
$$\frac{z_0}{R_p^2}\exp(-jkR_p)\times\exp\left[jk\sin\theta(x'\cos\phi+y'\sin\phi)\right]dx'dy' \quad (25a)$$

$$F_x = -\frac{\mu I_0}{8\pi^2 R}\exp(-jkR)\int_S \frac{\zeta^+\gamma z_0}{\zeta^+\gamma z_0+\alpha(y'-y_0)^2+\beta R_p^2}\left(\frac{\alpha(y'-y_0)^2}{R_p^2}+\beta\right)$$
$$\frac{\exp(-jkR_p)}{R_p}\times\exp\left[jk\sin\theta\left(x'\cos\phi+y'\sin\phi\right)\right]dx'dy' \quad (25b)$$

$$F_y = \frac{\mu I_0}{8\pi^2 R}\exp(-jkR)\int_S \frac{\zeta^+\gamma z_0}{\zeta^+\gamma z_0+\alpha(y'-y_0)^2+\beta R_p^2}\alpha\frac{(x'-x_0)(y'-y_0)}{R_p^3}$$
$$\exp(-jkR_p)\times\exp\left[jk\sin\theta(x'\cos\phi+y'\sin\phi)\right]dx'dy' \quad (25c)$$

3.4.3. z-directed Dipole

The incident vector potential

$$A_z^i = \frac{I_0}{4\pi}\frac{\exp(-jkR_p)}{R_p} \quad (26)$$

The current densities are

$$\mathbf{M} = \frac{\zeta^+\gamma}{\alpha z_0-\zeta^+\gamma}\frac{jkZ_0I_0}{2\pi}\left\{\frac{\hat{y}(x'-x_0)(z_0)-\hat{x}(y'-y_0)(z_0)}{R_p^2}\alpha\right\}$$
$$\frac{\exp(-jkR_p)}{R_p} \quad (27a)$$

$$\mathbf{J} = \frac{\alpha z_0}{\alpha z_0-\zeta^+\gamma}\frac{I_0}{2\pi}\left[-\hat{y}(y'-y_0)-\hat{x}(x'-x_0)\right]\left[jk+\frac{1}{R_p}\right]$$
$$\frac{\exp(-jkR_p)}{R_p^2} \quad (27b)$$

The corresponding vector potentials are

$$A_x = -\frac{\mu I_0}{8\pi^2 R}\exp(-jkR)\int_S \frac{\alpha z_0}{\alpha z_0-\zeta^+\gamma}\left[jk+\frac{1}{R_p}\right]\frac{(x'-x_0)}{R_p^2}$$
$$\exp(-jkR_p)\times\exp\left[jk\sin\theta(x'\cos\phi+y'\sin\phi)\right]dx'dy' \quad (28a)$$

$$A_y = -\frac{\mu I_0}{8\pi^2 R}\exp(-jkR)\int_S \frac{\alpha z_0}{\alpha z_0-\zeta^+\gamma}\left[jk+\frac{1}{R_p}\right]\frac{(y'-y_0)}{R_p^2}$$
$$\exp(-jkR_p)\times\exp\left[jk\sin\theta(x'\cos\phi+y'\sin\phi)\right]dx'dy' \quad (28b)$$

$$F_x = -\frac{\mu I_0}{8\pi^2 R}\exp(-jkR)\int_S \frac{\zeta^+\gamma}{\alpha z_0-\zeta^+\gamma}\frac{\alpha(y'-y_0)(z_0)}{R_p^3}\exp(-jkR_p) \times \exp\left[jk\sin\theta(x'\cos\phi+y'\sin\phi)\right]dx'dy' \quad (28c)$$

$$F_y = \frac{\mu I_0}{8\pi^2 R}\exp(-jkR)\int_S \frac{\zeta^+\gamma}{\alpha z_0-\zeta^+\gamma}\alpha\frac{(x'-x_0)(z_0)}{R_p^3}\exp(-jkR_p) \times \exp\left[jk\sin\theta(x'\cos\phi+y'\sin\phi)\right]dx'dy' \quad (28d)$$

Far field is obtained from the relation $E_\theta = -j\omega[A_\theta + Z_0F_\phi]$ and $E_\phi = -j\omega[A_\phi - Z_0F_\theta]$ where $A_\theta = A_x\cos\theta\cos\phi + A_y\cos\theta\sin\phi$ and $A_\phi = -A_x\sin\phi + A_y\cos\phi$.

4. RESULTS AND DISCUSSION

To investigate the dipole field scattering characteristics of impedance disk, expansion coefficients $A_{mn} \sim D_{mn}$ needs to be determined. These are determined through numerical computations and we have taken $m, n = 2 * \kappa$. The theoretical expressions for the far field are given by (19) for the impedance disk. The dipole is placed at $2.5\lambda_0$ and in xz-plane ($\phi_0 = 0$). Fig. 2 to Fig. 13 show the far field patterns of the impedance disk in the ϕ-cut plane $\phi = 0, \pi$ for ρ-, ϕ-, and z-directed dipole for different angle of incidence, disk sizes and surface impedances. The normalized disk sizes are $\kappa = ka = 3$, $ka = 5$ and, $ka = 7$ respectively. In all these figures, the normal incidence is for $\theta_0 = 0$. In all results, the value of surface impedance ($\zeta = 0.3 - j0.1$) is used except where the results are shown for different values of surface impedances which are mentioned in figures explicitly. In these figures, the field patterns obtained using the physical optics (PO) method are also included for comparison. The PO results are obtained using

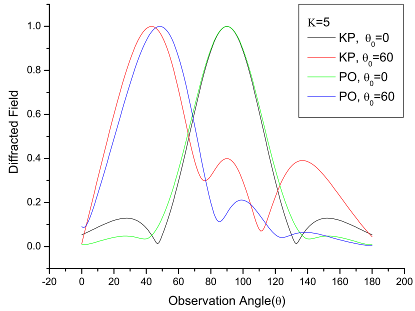

Figure 2. Comparison of KP and PO methods for ρ-directed dipole.

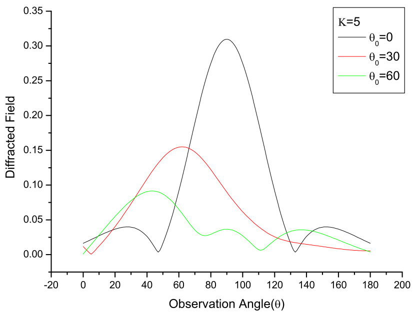

Figure 3. Field patterns for different incident angles for ρ-directed dipole.

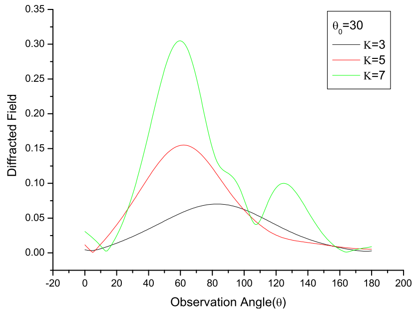

Figure 4. Field patterns for different disk sizes for ρ-directed dipole.

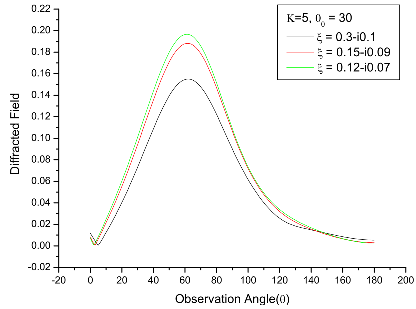

Figure 5. Field patterns for different surface impedances for ρ-directed dipole.

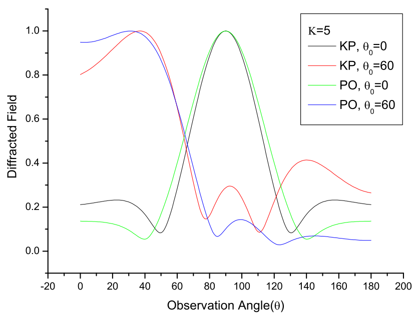

Figure 6. Comparison of KP and PO methods for ϕ-directed dipole.

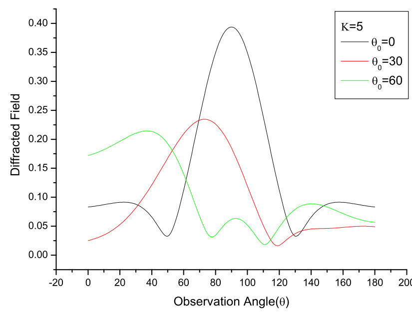

Figure 7. Field patterns for diffrent incident angles for ϕ-directed dipole.

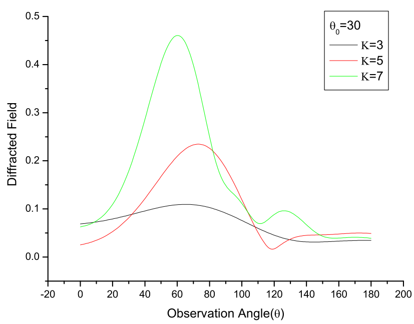

Figure 8. Field patterns for different disk sizes for ϕ-directed dipole.

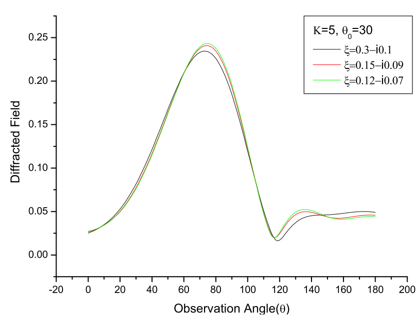

Figure 9. Field patterns for different surface impedances for ϕ-directed dipole.

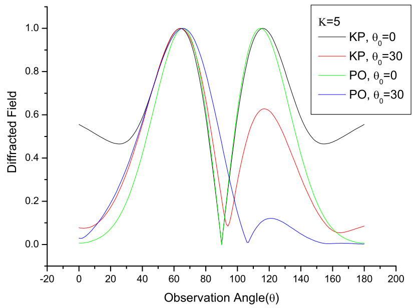

Figure 10. Comparison of KP and PO methods for z-directed dipole.

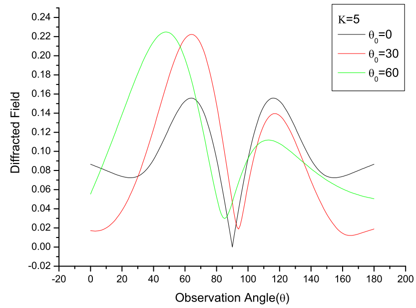

Figure 11. Field patterns for different incident angles for z-directed dipole.

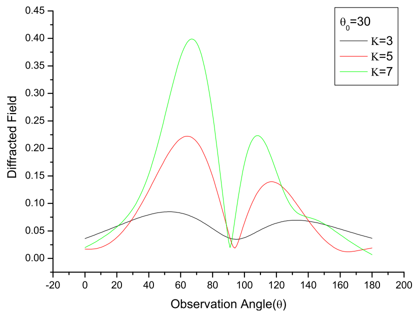

Figure 12. Field patterns for different disk sizes for z-directed dipole.

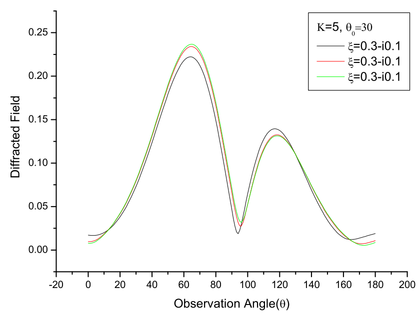

Figure 13. Field patterns for different surface impedances for z-directed dipole.

(22) $\sim$ (28). It is observed from the comparison that the PO and KP results agree well for normal incidence ($\theta_0 = 0$) but the degree of discrepancy increases as the angle of incidence becomes large. It is due to the fact that the PO approximation inaccuracy increases for shadow region contribution. The values of the normalized surface impedance ζ (0.3-j0.1, 0.15-j0.09, 0.12-j0.07) are taken from [42] which correspond to 5%, 10%, and 20% respectively gravimetric moisture content in San Antonio Gray Clay Loam with a density of $1.4\,\mathrm{g/cm^3}$. We also observe that the scattered field increases as the surface impedance of the disk decreases and it approaches to perfect electric conductor (PEC) disk scattering [23] case as the surface impedance leads to zero, as expected. Because PEC boundary condition is a special case of surface impedance boundary condition. But we see that this effect is more pronounced for ρ-directed dipole as compared to ϕ-directed dipole. We observe

through Figs. 3, 7 and 11 that the peak of the field patterns shifts as the incidence angle changes and the side lobes become more prominent as we increase the incidence angle.

ACKNOWLEDGMENT

This work has been funded by Higher Education Commission (HEC) of Pakistan.

REFERENCES

1. Senior, T. B. A., "Impedance boundary conditions for imperfectly conducting surfaces," *Appl. Sci. Res.*, Vol. 8, 418–436, 1960.
2. Shchukin, A. N., *Propagation of Radio Waves*, Svyazizdat, Moscow, Russia, 1940.
3. Leontovich, M. A., "Methods of solution for problems of electromagnetic waves propagation along the Earth surface," *Bull. Acad. Sci. USSR, Phys. Ser.*, Vol. 8, No. 1, 1622, 1944 (in Russian).
4. Pelosi, G. and P. Y. Ufimtsev, "The impedance-boundary condition," *IEEE Antennas Propag. Mag.*, Vol. 38, No. 1, 3135, Feb. 1996.
5. Lindell, I. V. and A. H. Sihvola, "Realization of impedance boundary," *IEEE Transactions on Antennas and Propagation*, Vol. 54, No. 12, 3669–3676, Dec. 2006.
6. Miller, R. F., "An approximate theory of the diffraction of an electromagnetic wave by an aperture in a plane screen," *Proc. IEE*, Vol. 103C, 177–185, 1956.
7. Miller, R. F., "The diffraction of an electromagnetic wave by a circular aperture," *Proc. IEE*, Vol. 104C, 87–95, 1957.
8. Lancellotti, V., B. P. de Hon, and A. G. Tijhuis, "Scattering from large 3-D piecewise homogeneous bodies through linear embedding via Green's operators and Arnoldi basis functions," *Progress In Electromagnetics Research*, Vol. 103, 305–322, 2010.
9. Shore, R. A. and A. D. Yaghjian, "Comparison of high frequency scattering determined from po fields enhanced with alternative ILDCs," *IEEE Transactions on Antennas and Propagation*, Vol. 52, 336–341, 2004.
10. Keller, J. B., "Geometrical theory of diffraction," *J. Opt. Soc. Amer.*, Vol. 52, No. 2, 116–130, Feb. 1962.
11. Moschovitis, C. G., H. Anastassiu, and P. V. Frangos, "Scattering

of electromagnetic waves from a rectangular plate using an extended stationary phase method based on Fresnel functions (SPM-F)," *Progress In Electromagnetics Research*, Vol. 107, 63–99, 2010.

12. Li, L. W., P. S. Kooi, Y. L. Qiu, T. S. Yeo, and M. S. Leong, "Analysis of electromagnetic scattering of conducting circular disk using a hybrid method," *Progress In Electromagnetics Research*, Vol. 20, 101–123, 1998.
13. Bouwkamp, C. J., "On the diffraction of electromagnetic wave by circular disks and holes," *Philips Res. Rep.*, Vol. 5, 401522, 1950.
14. Flammer, C., "The vector wave function solution of the diffraction of electromagnetic waves by circular discs and apertures — II, The diffraction problems," *J. Appl. Phys.*, Vol. 24, 1224–1231, 1953.
15. Bjrkberg, J. and G. Kristensson, "Electromagnetic scattering by a perfectly conducting elliptic disk," *Can. J. Phys.*, Vol. 65, 723–734, 1987.
16. Kristensson, G., "The current distribution on a circular disc," *Can. J. Phys.*, Vol. 63, 507–516, 1985.
17. Kristensson, G. and P. C. Waterman, "The T matrix for acoustic and electromagnetic scattering by circular disks," *J. Acoust. Soc. Am.*, Vol. 72, No. 5, 1612–1625, Nov. 1982.
18. Kristensson, G., "Natural frequencies of circular disks," *IEEE Transactions on Antennas and Propagation*, Vol. 32, No. 5, May 1984.
19. Balaban, M. V., R. Sauleau, T. M. Benson, and A. I. Nosich, "Dual integral equations technique in electromagnetic wave scattering by a thin disk," *Progress In Electromagnetics Research B*, Vol. 16, 107–126, 2009.
20. Nomura, Y. and S. Katsura, "Diffraction of electric wave by circular plate and circular hole," *Sci. Rep., Inst., Electr. Comm.*, Vol. 10, 1–26, Tohoku University, 1958.
21. Hongo, K. and Q. A. Naqvi, "Diffraction of electromagnetic wave by disk and circular hole in a perfectly conducting plane," *Progress In Electromagnetic Research*, Vol. 68, 113–150, 2007.
22. Inawashiro, S., "Diffraction of electromagnetic waves from an electric dipole by a conducting circular disk," *J. Phys. Soc. Japan*, Vol. 18, 273–287, 1963.
23. Hongo, K., A. D. U. Jafri, and Q. A. Naqvi, "Scattering of electromagnetic spherical wave by a perfectly conducting disk," *Progress In Electromagnetics Research*, Vol. 129, 315–343, 2012.
24. Jafri, A. D. U., Q. A. Naqvi, and K. Hongo, "Scattering

of electromagnetic plane wave by a circular disk with surface impedance," *Progress In Electromagnetics Research*, Vol. 127, 501–522, 2012.

25. Sebak, A. and L. Shafai, "Scattering from arbitrarily-shaped objects with impedance boundary conditions," *IEE Proceedings H*, Vol. 136, Part H, No. 5, Oct. 1989.
26. Bowman, J. J., T. B. A. Senior, and P. L. E. Uslenghi, *Electromagnetic and Acoustic Scattering from Simple Shapes*, North-Holland Publication Co., Amsterdam, 1969.
27. Balanis, C. A., *Antenna Theory Analysis and Design*, John Wiley & Sons, 1982.
28. Harrington, R. F., *Field Computation by Moment Methods*, Krieger Publication Co., Florida, 1968.
29. Kobayashi, I., "Darstellung eines potentials in zylindrical koordinaten, das sich auf einer ebene unterwirft," *Science Reports of the Thohoku Imperifal Unversity*, Ser. I, Vol. XX, No. 2, 197–212, 1931.
30. Sneddon, I. N., *Mixed Boundary Value Problems in Potential Theory*, North-Hollnd Publition Co., 1966.
31. Chew, W. C. and J. A. Kong, "Resonance of non-axial symmetric modes in circular microstrip disk antenna," *J. Math. Phys.*, Vol. 21, No. 3, 2590–2598, 1980.
32. Ding, D.-Z. and R.-S. Chen, "Electromagnetic scattering by conducting bor coated with chiral media above a lossy half-space," *Progress In Electromagnetics Research*, Vol. 104, 385–401, 2010.
33. Ji, W.-J. and C.-M. Tong, "Bistatic scattering from two-dimensional dielectric ocean rough surface with a PEC object partially embedded by using the g-smcg method," *Progress In Electromagnetics Research*, Vol. 105, 119–139, 2010.
34. Baussard, A., M. Rochdi, and A. Khenchaf, "PO/mec-based scattering model for complex objects on a sea surface," *Progress In Electromagnetics Research*, Vol. 111, 229–251, 2011.
35. Watson, G. N., *A Treatise on the Theory of Bessel Functions*, Cambridge at the University Press, 1944.
36. Magunus, W., F. Oberhettinger, and R. P. Soni, *Formulas and Theorems for the Spherical Functions of Mathematical Physics*, Springer Verlag, 1966.
37. Gradshteyn, I. S. and I. W. Ryzhik, *Table of Integrals, Series and Products*, Academic Press Inc., 1965.
38. Braver, I., P. Fridberg, K. Garb, and I. Yakover, "The behavior of the electromagnetic field near the edge of a resistive half-plane,"

IEEE Transactions on Antennas and Propagation,, Vol. 36, 1760–1768, 1988.

39. Meixner, J., "The behavior of electromagnetic fields at edges," *IEEE Transactions on Antennas and Propagation*, Vol. 20. No. 4. 442–446, Jul. 1972.
40. Hurd, R. A., "The edge condition in electromagnetics," *IEEE Transactions on Antennas and Propagation*, Vol. 24, No. 1, 70–73, Jan. 1976.
41. Illahi, A. and Q. A. Naqvi, "Scattering of an arbitrarily oriented dipole field by an infinite and finite length PEMC circular cylinder," *Central European Journal of Physics*, 829–853, 2009.
42. Sarabandi, K., M. D. Casciato, and I.-S. Koh, "Efficient calculation of the fields of a dipole radiating above an impedance surface," *IEEE Transactions on Antennas and Propagation*, Vol. 50, No. 9, 1222–1235, Sep. 2002.